

Age-related structural abnormalities in the human retina-choroid complex revealed by two-photon excited autofluorescence imaging

Meng Han

University of Heidelberg
Mannheim Biomedical Engineering Laboratories
Faculty of Clinical Medicine
Heidelberg, Germany
and
University of Heidelberg
Kirchhoff Institute for Physics
Heidelberg, Germany

Guenter Giese

Max-Planck Institute for Medical Research
Heidelberg, Germany

Steffen Schmitz-Valckenberg

Almut Bindewald-Wittich

Frank G. Holz

University of Bonn
Department of Ophthalmology
Bonn, Germany

Jiayi Yu

Josef F. Bille

University of Heidelberg
Kirchhoff Institute for Physics
Heidelberg, Germany

Markolf H. Niemz

University of Heidelberg
Mannheim Biomedical Engineering Laboratories
Faculty of Clinical Medicine
Heidelberg, Germany

1 Introduction

Vertebrate retinas share a common inverted structure, i.e., the photoreceptor layer is located at the far-most position in respect to incident light. Although the inverted arrangement seems unfavorable at first sight (the light has to travel through the whole neurosensory retina to reach photoreceptors), it is vital for the retina to survive in an environment with high photon and oxygen flux. The opaque layers, i.e., the retinal pigment epithelium (RPE) and the choroid, are indispensable to maintain the normal metabolism and visual function of the retina.^{1,2} RPE cells are highly specialized cells that serve as nurse cells for the retina with multiple essential functions.^{1,2} First, RPE digests the shed photoreceptor outer segments on a daily basis, transforms the photoisomerized all-*trans*-retinal back into 11-*cis*-retinal, and maintains the excitability of pho-

Abstract. The intensive metabolism of photoreceptors is delicately maintained by the retinal pigment epithelium (RPE) and the choroid. Dysfunction of either the RPE or choroid may lead to severe damage to the retina. Two-photon excited autofluorescence (TPEF) from endogenous fluorophores in the human retina provides a novel opportunity to reveal age-related structural abnormalities in the retina-choroid complex prior to apparent pathological manifestations of age-related retinal diseases. In the photoreceptor layer, the regularity of the macular photoreceptor mosaic is preserved during aging. In the RPE, enlarged lipofuscin granules demonstrate significantly blue-shifted autofluorescence, which coincides with the depletion of melanin pigments. Prominent fibrillar structures in elderly Bruch's membrane and choriocapillaries represent choroidal structure and permeability alterations. Requiring neither slicing nor labeling, TPEF imaging is an elegant and highly efficient tool to delineate the thick, fragile, and opaque retina-choroid complex, and may provide clues to the trigger events of age-related macular degeneration. © 2007 Society of Photo-Optical Instrumentation Engineers. [DOI: 10.1117/1.2717522]

Keywords: two-photon imaging; autofluorescence; retina; choroid.

Paper 06220R received Aug. 11, 2006; revised manuscript received Dec. 29, 2006; accepted for publication Jan. 2, 2007; published online Apr. 18, 2007.

toreceptors. Second, RPE takes up and delivers nutrients to the neurosensory retina and transports the metabolic end products to the choroid. Third, RPE has elaborate mechanisms to remove the toxic molecules and free radicals produced by the light, contributing to a stable and optimum retinal environment. Fourth, the melanin pigment in the RPE protects the photoreceptors from short-wavelength light damage and shields scattered light from the sclera. The intensive metabolic activities in the RPE require a good blood supply, which is provided by the choroid being in intimate contact with the RPE. The choroid is the layer that actively transports the metabolic waste and nutrients from and to the photoreceptors, respectively.³ The choroid takes approximately 85% of the ocular blood flow and is remarkable for its high blood flow rate. Besides its transport function, the choriocapillaries act as a heat sink to reduce subretinal temperature and photochemical injury to the RPE.⁴ A failure of the functions of either RPE

Address all correspondence to Meng Han, Kirchhoff Institute for Physics, INF. Tel: 0049-6221-549254; Fax: 0049-6221-549112; E-mail: mhan@urz.uni-heidelberg.de

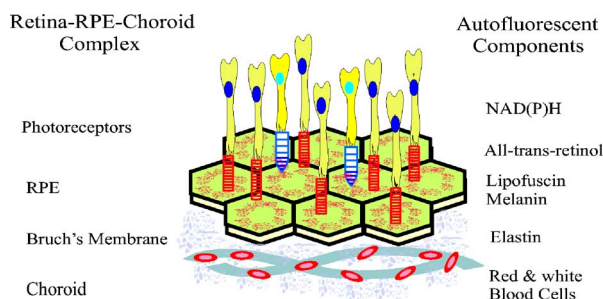


Fig. 1 Endogenous chromophores in the human photoreceptor-RPE-choroid complex. The major fluorophore in the outer segment of the photoreceptor is all-*trans*-retinol. NAD(P)H is located in the photoreceptor inner segment and in the outer nuclear layer. Lipofuscin and melanin are the predominant fluorophores in the RPE. The Bruch's membrane and choriocapillaries can be delineated based on the autofluorescence of elastin, and red/white blood cells.

or choroid may lead to degeneration of photoreceptors, impairment in visual acuity, and eventually to blindness.

Age-related macular degeneration (AMD) is the principal cause of irreversible loss of vision and registered legal blindness for aging people in developed countries. To place this in perspective, 35% of the human population older than 75 years have some degree of AMD.^{5,6} AMD is characterized by the progressive degeneration of photoreceptors, RPE, and choroid.^{7,8} The earliest visible abnormality in AMD is the extracellular accumulation of drusen (waste material) underneath the RPE cell monolayer. Despite extensive research, the trigger events and the primary injury sites of AMD have always been subjects of considerable debate. Fundamentally, there are two hypotheses regarding the primary cause of AMD.⁵ One claims a vascular origin associated with an imbalance between angiogenetic and antiangiogenetic factors. The second suggests that dysfunction of the RPE is responsible for AMD. The development of AMD is thought to result from an accentuation of the aging process, since most of the structural abnormalities presented in AMD are also observed in normal aged eyes. A noninvasive, high resolution, and large sensing depth imaging modality is vital to delineate the age-related structural abnormalities in the fragile, pigmented retina-choroid complex and to provide clues to the events that transform normal aging processes into early AMD developments.

Although for most imaging applications autofluorescence is a source of background and may need to be suppressed, autofluorescence is particularly valuable in ophthalmology and has been successfully used for diagnostic *in-vivo* autofluorescence imaging as well as for experimental *ex-vivo* imaging techniques.⁹⁻¹⁴ As illustrated in Fig. 1, the human retina appears to be an ideal target for endogenous fluorescence imaging. The major autofluorescent sources in human retina include all-*trans*-retinol and NAD(P)H in photoreceptors, lipofuscin and melanin in the RPE, elastin in Bruch's membrane, and red/white blood cells in choroid. All of them are among the most vital components in the retina-choroid complex. However, the most effective excitation light for the retinal autofluorescence is in the blue-UV range, which is either strongly scattered or absorbed in the opaque RPE-choroid complex and may induce severe photodamage. The advan-

tages of autofluorescence retinal imaging cannot be appreciated with conventional single-photon imaging. The advent of ultra-fast pulsed laser sources allowed the use of a nonlinear absorption process for two-photon microscopic fluorescence imaging.^{15,16} Near-infrared (NIR) ultra-fast lasers are employed as the excitation light source, resulting in largely increased sensing depth and reduced photodamage.¹⁷⁻²² As a second-order effect, two-photon absorption is confined within the central focus of the illuminating beam. Lateral and depth discrimination are achievable without extra confocal pinholes,²³ permitting 3-D optical sectioning of thick retina-choroid complex. Although two-photon excited fluorescence (TPEF) imaging has been extensively applied in neurophysiology, developmental biology, and biopsy,¹⁹⁻²⁵ TPEF ophthalmic imaging is still in the early development stage.²⁵⁻³⁶ To the best of our knowledge, we are the first to employ two-photon excited autofluorescence imaging to resolve the age-related structural abnormalities in the human retina-choroid complex prior to apparent pathological manifestations of AMD. As a simple and efficient method, TPEF imaging has tremendous potential in delineating the cellular structures of retina-choroid complex, and may provide fresh insights into the pathogenesis of blinding retinal diseases.

2 Materials and Methods

2.1 Human Retina Samples

Retinas were obtained from four human Caucasian postmortem donor eyes (19, 55, 57, and 64 years old, with normal vision) from the eye bank of the Department of Ophthalmology, University of Bonn, Germany. Informed consent to cornea transplantation and further use of tissue for research was obtained from a relative of the donors or documented in an organ donor pass in accordance with German law for organ donation. In all of the four donor eyes, there were no macroscopic visible retinal abnormalities such as soft drusen, retinal hemorrhage, or choroidal neovascularization. After enucleation, the eyeballs were cut equatorially and fixed with paraformaldehyde [4% in phosphate buffered saline (PBS), pH 7.4].

2.2 Two-Photon Excited Autofluorescence Imaging

In this study, TPEF imaging was performed on a customized upright laser scanning microscope (Zeiss LSM 510 NLO, Zeiss, Jena, Germany) equipped with a femtosecond Ti:sapphire laser (Coherent Chameleon XR, Coherent Incorporated, Santa Clara, California). The wavelength of the 90-MHz, 150 fs Ti:sapphire laser pulses is tunable from 705 to 980 nm. A 5-mm-diam retina/sclera tissue probe in the macular region was manually prepared with a surgical trephine. First, the neurosensory retina then the RPE were carefully removed from the tissue probe, allowing high resolution imaging of photoreceptors, RPE, and choroid, respectively. All prepared tissue specimens were transferred to a custom-made tissue dish filled with PBS (pH 7.4) solution and imaged with a large working distance water-immersion objective (Zeiss, 63 \times , NA 1.0). The average laser power at the back focal plane of the objective was attenuated below \sim 4 mW for RPE imaging and was kept between 4 mW \sim 10 mW for 3D photoreceptor and choroid imaging, which are close to the previously reported damage thresholds.^{35,36} We did not observe no-

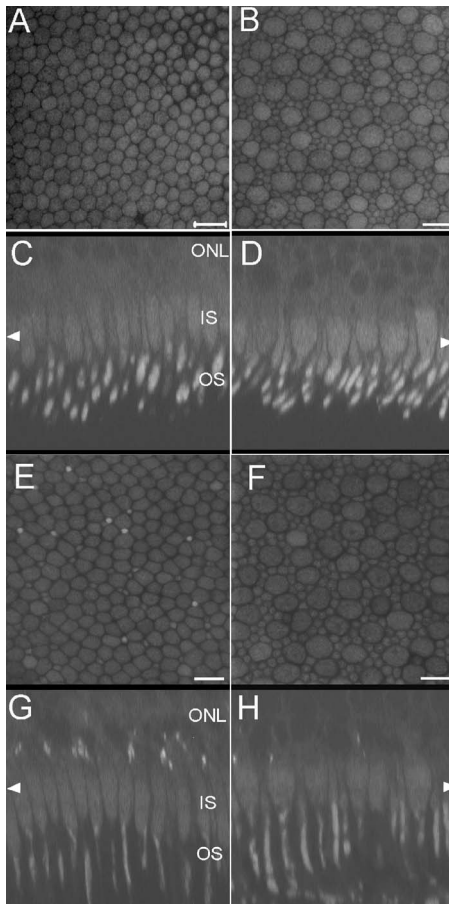


Fig. 2 Human cone and rod photoreceptor mosaic delineated by TPEF imaging. (a) and (b) Cone and rod mosaic in fovea, parafovea (1.2-mm eccentricity) of the 19-year-old eye. (c) and (d) Cross section images of foveal, parafoveal photoreceptors of the 19-year-old eye. The locations of the optical slices of (a) and (b) are indicated by the arrowheads in (c) and (d). (e) through (h) Corresponding single slice and cross section images of the 57-year-old photoreceptors in fovea and parafovea (1.2-mm eccentricity), respectively. ONL is the photoreceptor outer nuclear layer; IS is the inner segments; and OS is the outer segments. Scale bar, 10 μm .

ticeable photodamages to the fixed retina during imaging. Through a set of dichroic beamsplitters, the autofluorescence signals were detected by photomultiplier tubes assigned to different spectral windows, namely, 500 to 550 nm for photoreceptor imaging (Fig. 2), 435 to 485 and 515 to 700 nm for RPE-choroid-Bruch's membrane imaging [Figs. 3, 4(b), and 5], and 500 to 550 and 575 to 640 nm for lipofuscin and melanin imaging [Fig. 4(a)]. The wavelength of the Ti:sapphire laser for TPEF imaging was set to 800 nm, except for Fig. 4(a) (916 nm). The cross section images of photoreceptors in Figs. 2(c) and 2(d), and Figs. 2(g) and 2(h) were reconstructed from 70- μm -depth image stacks with slice intervals of 1 μm .

3 Results

3.1 Aging of Cone and Rod Photoreceptors Revealed by Two-Photon Excited Autofluorescence Imaging

As shown in Fig. 2, individual cones and rods were clearly resolved with TPEF imaging, requiring neither slicing nor la-

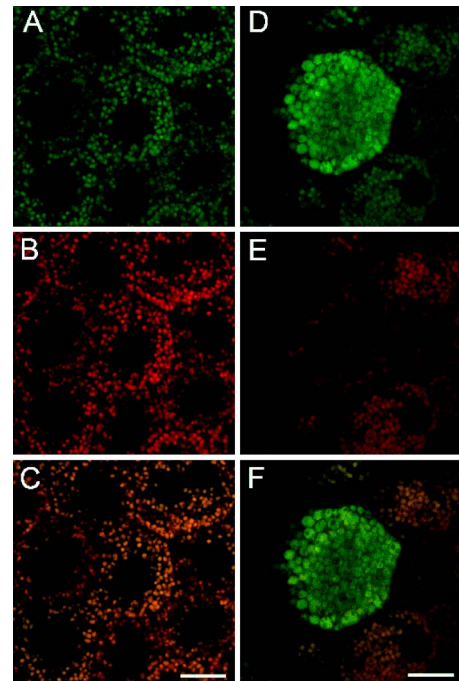


Fig. 3 Morphometric and spectral characterizations of single lipofuscin granules in human RPE cells. TPEF signals from the 19-year-old macular RPE cells were acquired with two spectral windows color coded in (a) green ($435 < \lambda_{AF} < 485 \text{ nm}$) and (b) red ($515 < \lambda_{AF} < 700 \text{ nm}$). (c) Merged TPEF images of the 19-year-old RPE cells. (d), (e), and (f) Corresponding TPEF images of the 64-year-old macular RPE cells (green channel and red channel, merged, color online only), respectively. Large lipofuscin granules in the 64-year-old eye demonstrate significantly blue-shifted autofluorescence. Scale bar, 10 μm .

beling. In the fovea of the 19-year-old retina, the cone mosaic exhibits an impressive hexagonal symmetry [Fig. 2(a)]. In the parafovea, enlarged cones are surrounded by rods of uniform size and density [Fig. 2(b)]. The rod-to-cone ratio is approximately 9:1 in the parafovea. Since the sensing depth of TPEF imaging exceeds 100 μm , the full depth of photoreceptors, including outer segments, inner segments, and outer nuclear layer, can be delineated. Although several retinoid metabolites

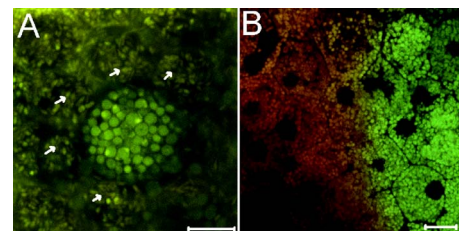


Fig. 4 (a) Interdependence of melanin and lipofuscin pigment granules in the RPE. Most of the melanin pigment granules (as indicated by the arrows) are located in the apical pole of the RPE cells. In the RPE cells (55 year old), which contain enlarged lipofuscin granules with blue-shifted autofluorescence, the amount of melanin granules decreased remarkably. (b) Blue-light irradiation elicits autofluorescence shift of lipofuscin granules in the RPE (64 year old). Compared with the normal RPE cells on the left, the blue-light-illuminated RPE cells on the right demonstrate significantly blue-shifted autofluorescence. Scale bar, 10 μm .

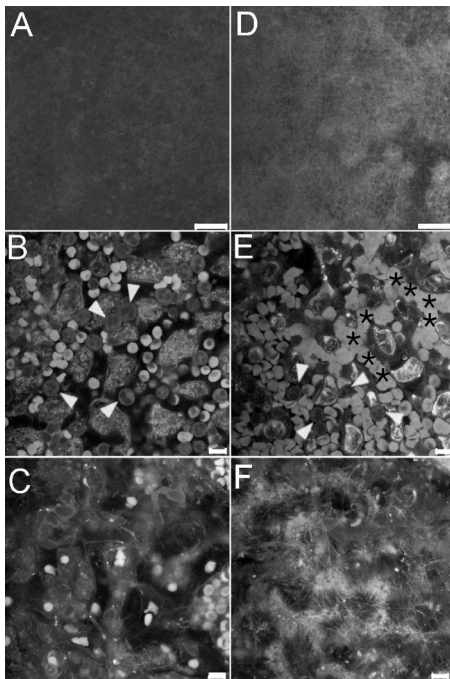


Fig. 5 Age-related choroidal structural and circulation alterations. Bruch's membrane [(a) and (d)] and choriocapillaries [(b) and (e)] in the 19- and 64-year-old choroids, respectively. Black asterisks: jammed red blood cells. White arrowheads: representative white blood cells (neutrophils). (c) and (f) The choroidal layer immediately underneath the choriocapillaries. The interwoven fibrous structures are present in (f) the 64-year-old choroid, but not in (c) the 19-year-old choroid. Scale bar, 10 μm .

are generated in the photoreceptors, only all-*trans*-retinol shows intrinsic fluorescence.³⁷ As illustrated in the optical cross section images in Figs. 2(c) and 2(d), the brightest autofluorescence is located at the photoreceptor outer segments, where the all-*trans*-retinol is derived from the visual cycle.³⁸ The weaker autofluorescence in the photoreceptor inner segments is supposed to be generated by NAD(P)H in the photoreceptor mitochondrias.³⁷ Rod and cone outer segments exhibit similar brightness, indicating a comparable concentration of all-*trans*-retinol in both types of photoreceptors. In the 57-year-old retina, the size and length of the photoreceptor outer segments are more variable. However, the regularity of the photoreceptor mosaic and the average densities of rod and cone photoreceptors are preserved in both fovea and parafovea. In the region between the photoreceptor inner segments and the outer nuclear layer, strongly autofluorescent intracellular inclusions were delineated [Figs. 2(g) and 2(h)]. They were predominantly located in the aged cones and were not observed in the 19-year-old photoreceptors.

3.2 Two-Photon Excited Autofluorescence Imaging of Individual Lipofuscin Granules in Human Retinal Pigment Epithelium Cells

One of the major fluorophores in the RPE is N-retinylidene-N-retinylethanolamine (A2E), an orange fluorescent pyridinium bisretinoid, which is derived from two molecules of all-*trans*-retina.³⁹⁻⁴² A2E accumulates in the RPE during phagocytosis of the photoreceptor outer segments and is taken

up by lysosomes. Once formed, A2E cannot be naturally degraded and may condensate in the lipofuscin granules. The excess accumulation of lipofuscin is deleterious for RPE.⁴³⁻⁴⁶ Lipofuscin is phototoxic, may interfere with lysosomal degradation, and trigger RPE cell apoptosis.⁴³⁻⁴⁶ Characterization of the lipofuscin granules in the RPE is crucial to understanding the aging process and the pathogenesis of complex retinal diseases such as AMD and monogenetic juvenile macular dystrophies, including Stargardt or Best disease, which are associated with excessive accumulation of lipofuscin. As shown in Fig. 3, lipofuscin granules in the 19-year retina are preferably located adjacent to the RPE cell membranes. The typical diameter of lipofuscin granules is close to 1 μm ; smaller or larger lipofuscin granules are few. In the 64-year-old retina, the majority of the RPE cytoplasm tends to be occupied by lipofuscin granules. In addition to the established methods such as mass spectrometry and Western blot analysis,^{47,48} the intricate composition of RPE and lipofuscin granules can be probed by fluorescence spectral imaging. As shown in Fig. 3, the autofluorescence of RPE is detected with two color-coded spectral windows. Lipofuscin (LF) granules exhibiting enhanced green fluorescence are immediately identified, which appear unusually large and are confined within individual, sparse RPE cells. Our previous investigations revealed that the autofluorescence emission peak of these large-type LF granules is located at 520 nm, which is significantly blue-shifted compared with the autofluorescence peak (556 nm) of normal LF granules.^{32,33} The large-type lipofuscin granules are relatively rare ($\approx 0.1\%$). They were commonly observed in the aging donor eyes (55, 57, and 64-year-old RPE), but were not present in the 19-year-old RPE.

Further examination revealed a remarkable loss of typical melanin granules in these particular RPE cells [Fig. 4(a)]. Depletion of the photoprotection agent of melanin leads to elevated short-wavelength light exposure to RPE, which may be one possible cause for the abnormal autofluorescence from the corresponding lipofuscin granules. To prove this hypothesis, RPE cells containing lipofuscin granules with normal autofluorescence were exposed to blue-light radiation for two hours (Zeiss 50-W mercury lamp with Zeiss filter set 9). Significantly blue-shifted autofluorescence from the illuminated lipofuscin granules was observed [Fig. 4(b)]. However, whether the unusual autofluorescence of lipofuscin granules is associated with photo-oxidized lipofuscin/melanosome or other types of blue-light-induced photochemical reactions is beyond the scope of this work.⁴⁹

3.3 Age-Related Choroidal Structural Alterations

The accumulation of extracellular deposit at the retina-choroid interface alters Bruch's membrane composition and permeability, which may lead to impaired diffusion between RPE and choroid, and is thought to contribute to the pathogenesis of AMD.⁵⁰ In the wet-type AMD, choroidal neovascularization destroys the architecture of the outer retina and leads to sudden loss of central vision. It is important to characterize the age-related choroidal circulation and structure alterations prior to the abrupt neovascularization process.⁵¹⁻⁵⁴ As demonstrated in Fig. 5, the autofluorescence from elastin in Bruch's membrane/intercapillary pillars and from the red/white blood cells in the capillaries provides a noninvasive and

Table 1 Age-related structural abnormalities in the human retina-choroid complex.

Retina-choroid complex	Endogenous fluorophores	Age-related structural abnormalities
Photoreceptors	NAD(P)H All- <i>trans</i> -retinol	Autofluorescent intracellular inclusions in elderly cones. More variable outer segments with increasing age.
RPE	A2E Melanosome	Excessive accumulation of lipofuscin. Blue-shifted fluorescence from enlarged lipofuscin granules. Melanin depletion in RPE cells with blue-shifted fluorescence.
Bruch's membrane	Elastin Extracellular deposit	Significantly increased autofluorescence. Fibrillar structures in Bruch's membrane.
Choroid	Elastin White/red blood cells	Probable decrease in choroidal circulation. Fibrillar structures beneath choriocapillaries.

efficient way to characterize the Bruch's membrane and the choroid. Fibrous structures were observed in the 64-year-old Bruch's membrane [Fig. 5(d)], which was accompanied by a significant increase of the autofluorescence. TPEF imaging revealed a high density of choriocapillaries beneath Bruch's membrane [Figs. 5(b) and 5(c)]. Inside the choriocapillaries, white blood cells (10 to 12 μm in diameter) can be clearly distinguished from red blood cells (7 to 9 μm in diameter). Most of the blood cells appear to be neutrophils, which contain multiple nuclear lobes. The white-to-red blood cell ratio in the choriocapillaries ($>1:30$) is remarkably higher than the normal ratio ($\approx 1:600$). Strongly jammed red blood cells in the choriocapillaries [Fig. 5(e)] and prominent interwoven fibrillar structures immediately beneath the choriocapillaries [Fig. 5(f)] were observed in the elderly choroids (55- and 64-year-old) but were not found in the 19-year-old choroid [Figs. 5(b) and 5(c)].

4 Discussion

Based on the endogenous chromophores in the human retina-choroid complex, the age-related structural abnormalities (Table 1) in the photoreceptors, RPE cells, Bruch's membrane, and the choroid were successfully delineated with two-photon excited autofluorescence imaging *ex vivo*. Individual cones or rods were resolved based on the autofluorescence from all-*trans*-retinol and NAD(P)H in the photoreceptor outer and inner segments, respectively. As age increases, the average densities of rods and cones appear unchanged in both fovea and parafovea. Our observations are inconsistent with the previous morphometric studies, where the parafoveal rod loss is generally greater than foveal cone loss during aging.^{55,56} The discrepancy may result from the fact that all of the donor eyes under our investigations have normal vision and are younger than 64 years. Strongly autofluorescent intracellular inclusions were found in the aged cones. The origin of these autofluorescent inclusions and their influence to the visual function of the cones are worth further investigations. Derived from incompletely digested photoreceptor outer segments, lipofuscin accumulates in the RPE and exhibits the strongest autofluorescence in the retina. In the aged RPE, the amount of lipofuscin granules increases significantly. The average size of the lipofuscin granules remains more or less unchanged. However, individual RPE cells containing enlarged lipofuscin granules with strongly blue-shifted autofluo-

rescence were observed in the elderly RPE, which was accompanied by a significant reduction in the melanin content. In addition to its light absorption function, melanin may act as an antioxidant to protect the RPE from photo-oxidative stress.⁵⁷ The occurrence of blue-shifted lipofuscin autofluorescence coincides with the depletion of melanin pigments in the aged RPE, suggesting a complicated interdependence between lipofuscin and melanin in the RPE. In the choroid, autofluorescence from elastin and from red/white blood cells offers an unique opportunity to delineate Bruch's membrane, choriocapillaries, and intercapillary pillars. The elderly Bruch's membrane demonstrated a significant increase of autofluorescence, which may represent age-related accumulation of autofluorescent sub-RPE deposits.¹⁴ In the choroidal layer beneath Bruch's membrane, an extraordinary high density of choriocapillaries was resolved, which appears essential for the choroid to sustain a high blood circulation rate. A remarkably high white-to-red blood cell ratio was observed in the post-mortem choriocapillaries. Such a high white blood cell concentration may be advantageous for efficient digestion of the metabolic end products from retina through phagocytosis; however, whether it represents the status of the living eye needs to be verified through further *in-vivo* examinations. Previous studies have reported an age-related decrease in choroidal circulation,^{53,54} which is consistent with our *ex-vivo* observations that red blood cells tend to jam in the elderly choriocapillaries. In the fovea, the choroidal circulation is the only source of nourishment to the retina and is responsible for removal of metabolites from the fovea. The ability of the choroid to sustain a healthy environment in the fovea strongly depends on an ample choroidal blood flow. A decrease in the choroidal flow rate may have deleterious effects to the retina. Besides the choroidal circulation alterations, the presence of prominent fibrillar structures in Bruch's membrane and underneath the choriocapillaries is one of the most distinct characteristics of the elderly choroid. Such abnormalities in the extracellular matrix, plus age-related decrease in the choroidal blood flow, may impair the transport efficiency of the choriocapillaries, reduce the permeability of Bruch's membrane, and give rise to further RPE and photoreceptor damages.

As an elegant and highly efficient method, TPEF imaging is especially valuable to delineate the thick, fragile, and opaque human retina-choroid complex *ex vivo*. The most vital components (photoreceptors, RPE, choriocapillaries, Bruch's

membrane) in the human retina-choroid complex can be examined with subcellular resolution. Unlike conventional histological and electron micrographic methods,^{58,59} complicated and invasive procedures including labeling and slicing are unnecessary. Compared with other noninvasive methodologies like confocal imaging, TPEF is more appropriate to probe the opaque RPE-choroid complex, because the short-wavelength light, which is typically employed for single-photon fluorescence imaging, will be strongly absorbed in cornea, RPE, and choroid. Furthermore, based on the transparency of the eye to the NIR light, cellular events in the living retina may be unraveled by TPEF imaging. As demonstrated by an excellent recent study, TPEF imaging has huge potential in *in-vivo* imaging of the intact retina.²⁸ Better retina-choroid imaging modalities will accelerate progress in understanding the pathogenesis of AMD, and will help to design effective therapies for AMD at early stages of the disease. Without sacrificing the animals under investigation,⁵⁹ trigger events for retinal diseases and retinal degenerations, as well as possible regeneration processes under pharmaceutical interventions, may be monitored at the cellular level, and truly *in vivo*.⁶⁰

Acknowledgments

The authors are indebted to Winfried Denk for access to the microscopy facility of the Max-Planck Institute for Medical Research, Heidelberg, and to Simone Astori, Juergen Sawinski, and Annemarie Scherbarth for stimulating discussions. This work was supported by the MABEL Laboratory at the faculty of clinical medicine at Mannheim, University of Heidelberg, Germany.

References

- O. Strauss, "The retinal pigment epithelium in visual function," *Physiol. Rev.* **85**, 845–881 (2005).
- R. W. Young and D. Bok, "Participation of the retinal pigment epithelium in the rod outer segment renewal process," *J. Cell Biol.* **42**, 392–402 (1969).
- P. Toernquist, A. Alm, and A. Bill, "Permeability of ocular vessels and transport across the blood-retinal barrier," *Eye* **4**, 303–309 (1990).
- L. M. Parver, C. Auken, and D. O. Carpenter, "Choroidal blood flow as a heat dissipating mechanism in the macula," *Am. J. Ophthalmol.* **89**, 641–646 (1980).
- D. Bok, "New insights and new approaches toward the study of age-related macular degeneration," *Proc. Natl. Acad. Sci. U.S.A.* **99**, 14619–14621 (2002).
- R. Klein, B. E. Klein, and K. L. Linton, "Prevalence of age-related maculopathy. The Beaver Dam eye study," *Ophthalmology* **99**, 933–943 (1992).
- Z. A. Zarbin, "Current concepts in the pathogenesis of age-related macular degeneration," *Arch. Ophthalmol. (Chicago)* **122**, 598–614 (2004).
- P. V. Alverer and S. Seregard, "Age-related maculopathy: pathogenetic features and new treatment modalities," *Acta Ophthalmol. Scand.* **80**, 136–143 (2002).
- F. C. Delori et al., "*In vivo* fluorescence of the ocular fundus exhibits retinal pigment epithelium lipofuscin characteristics," *Invest. Ophthalmol. Visual Sci.* **36**, 718–729 (1995).
- F. C. Delori, G. Douglas, D. G. Goger, and C. K. Dorey, "Age-related accumulation and spatial distribution of lipofuscin in RPE of normal subjects," *Invest. Ophthalmol. Visual Sci.* **42**, 1855–1866 (2001).
- S. Schmitz-Valckenberg et al., "Fundus autofluorescence and fundus perimetry in the junctional zone of geographic atrophy in patients with age-related macular degeneration," *Invest. Ophthalmol. Visual Sci.* **45**, 4470–4476 (2004).
- A. Bindewald, J. J. Jorzik, A. Loesch, F. Schutt, and F. G. Holz, "Visualization of retinal pigment epithelial cells *in vivo* using digital high-resolution confocal scanning laser ophthalmoscopy," *Am. J. Ophthalmol.* **137**, 556–558 (2004).
- A. von Rückmann, F. W. Fitzke, and A. C. Bird, "Distribution of fundus autofluorescence with a scanning laser ophthalmoscope," *Br. J. Ophthalmol.* **79**, 407–412 (1995).
- A. D. Marmorstein, L. Y. Marmorstein, H. Sakaguchi et al., "Spectral profiling of autofluorescence associated with lipofuscin, Bruch's membrane, and sub-RPE deposits in normal and AMD eyes," *Invest. Ophthalmol. Visual Sci.* **43**, 2435–2441 (2002).
- C. J. R. Sheppard and R. Kompfner, "Resonant scanning optical microscope," *Appl. Opt.* **17**, 2879–2882 (1978).
- W. Denk, J. H. Strickler, and W. W. Webb, "Two-photon laser scanning fluorescence microscopy," *Science* **248**, 73–76 (1990).
- R. M. Williams, D. W. Piston, and W. W. Webb, "Two-photon molecular excitation provides intrinsic 3-dimensional resolution for laser-based microscopy and microphotochemistry," *FASEB J.* **8**, 804–813 (1994).
- W. R. Zipfel, R. M. Williams, R. Christie, A. Y. Nikitin, B. T. Hyman, and W. W. Webb, "Live tissue intrinsic emission microscopy using multiphotonexcited native fluorescence and second harmonic generation," *Proc. Natl. Acad. Sci. U.S.A.* **100**, 7075–7080 (2003).
- W. R. Zipfel, R. M. Williams, and W. W. Webb, "Nonlinear magic: multiphoton microscopy in the biosciences," *Nat. Biotechnol.* **21**, 1369–1377 (2003).
- P. J. Campagnola, H. A. Clark, W. A. Mohler, A. Lewis, and L. M. Loew, "Second-harmonic imaging microscopy for visualizing biomolecular arrays in cells, tissues and organisms," *Nat. Biotechnol.* **21**, 1356–1360 (2003).
- K. Koenig, "Multiphoton microscopy in life sciences," *J. Microsc.* **200**, 83–104 (2000).
- P. T. C. So, C. Y. Dong, B. R. Masters, and K. M. Berland, "Two-photon excitation fluorescence microscopy," *Annu. Rev. Biomed. Eng.* **2**, 399–429 (2000).
- F. Helmchen and W. Denk, "Deep tissue two-photon microscopy," *Nat. Methods* **2**, 932–940 (2005).
- W. Supatto et al., "*In vivo* modulation of morphogenetic movements in *Drosophila* embryos with femtosecond laser pulses," *Proc. Natl. Acad. Sci. U.S.A.* **102**, 1047–1052 (2005).
- K. A. Kasischke, H. D. Vishwasrao, P. J. Fisher, W. R. Zipfel, and W. W. Webb, "Neural activity triggers neuronal oxidative metabolism followed by astrocytic glycolysis," *Science* **305**, 99–103 (2004).
- A. T. Yeh, N. Nassif, A. Zoumi, and B. J. Tromberg, "Selective corneal imaging using combined second harmonic generation and two-photon excited fluorescence," *Opt. Lett.* **27**, 2082–2084 (2002).
- J. G. Lyubovitsky, J. A. Spencer, T. B. Krasieva, B. Andersen, and B. J. Tromberg, "Imaging corneal pathology in a transgenic mouse model using nonlinear microscopy," *J. Biomed. Opt.* **11**, 014013 (2006).
- Y. Imanishi, M. L. Batten, D. W. Piston, W. Baehr, and K. Palczewski, "Noninvasive two-photon imaging reveals retinyl ester storage structures in the eye," *J. Cell Biol.* **164**, 373–383 (2004).
- M. Han, L. Zickler, G. Giese, F. Loesel, M. Walter, and J. F. Bille, "Second harmonic corneal imaging after femtosecond laser surgery," *J. Biomed. Opt.* **9**, 760–766 (2004).
- M. Han, G. Giese, L. Zickler, H. Sun, and J. F. Bille, "Mini-invasive corneal surgery and imaging with femtosecond lasers," *Opt. Express* **12**, 4275–4281 (2004).
- M. Han, G. Giese, and J. F. Bille, "Second harmonic generation imaging of collagen fibrils in cornea and sclera," *Opt. Express* **13**, 5791–5795 (2005).
- M. Han et al., "Two-photon excited autofluorescence imaging of human retinal pigment epithelial cells," *J. Biomed. Opt.* **11**, 010501 (2006).
- A. Bindewald-Wittich et al., "Two photon excited fluorescence imaging of human RPE cells using a femtosecond Ti:sapphire laser," *Invest. Ophthalmol. Visual Sci.* **47**, 4553–4557 (2006).
- S. W. Teng et al., "Multiphoton autofluorescence and second-harmonic generation imaging of the *ex vivo* porcine eye," *Invest. Ophthalmol. Visual Sci.* **47**, 1216–1224 (2006).

35. K. Konig, T. W. Becker, P. Fischer, I. Riemann, and K. J. Halhuber, "Pulse-length dependence of cellular response to intense near-infrared laser pulses in multiphoton microscopes," *Opt. Lett.* **24**, 113–115 (1999).
36. A. Hopt and E. Neher, "Highly nonlinear photodamage in two-photo fluorescence microscopy," *Biophys. J.* **80**, 2029–2036 (2001).
37. C. Chen et al., "Reduction of all-trans retinal to all-trans retinol in the outer segments of frog and mouse rod photoreceptors," *Biophys. J.* **88**, 2278–2287 (2005).
38. J. C. Saari, "Biochemistry of visual pigment regeneration," *Invest. Ophthalmol. Visual Sci.* **41**, 337–348 (2000).
39. N. Sakai, J. Decatur, and K. Nakanishi, "Ocular age pigment A2-E: An unprecedented pyridinium bisretinoid," *J. Am. Chem. Soc.* **118**, 1559–1560 (1996).
40. N. L. Mata, J. Weng, and G. H. Travis, "Biosynthesis of a major lipofuscin fluorophore in mice and humans with ABCR-mediated retinal and macular degeneration," *Proc. Natl. Acad. Sci. U.S.A.* **97**, 7154–7159 (2000).
41. N. L. Mata et al., "Delayed dark-adaptation and lipofuscin accumulation in abcr+/- mice: Implications for involvement of ABCR in age-related macular degeneration," *Invest. Ophthalmol. Visual Sci.* **42**, 1685–1690 (2001).
42. J. R. Sparrow, "Therapy for macular degeneration: Insights from acne," *Proc. Natl. Acad. Sci. U.S.A.* **100**, 4353–4354 (2003).
43. F. G. Holz et al., "Inhibition of lysosomal degradative functions in RPE cells by a retinoid component of lipofuscin," *Invest. Ophthalmol. Visual Sci.* **40**, 737–743 (1999).
44. J. R. Sparrow, K. Nakanishi, and C. A. Parish, "The lipofuscin fluorophore A2E mediates blue light-induced damage to retinal pigmented epithelial cells," *Invest. Ophthalmol. Visual Sci.* **41**, 1981–1989 (2000).
45. F. Schuett, S. Davies, J. Kopitz, F. G. Holz, and M. E. Boulton, "Photodamage to human RPE cells by A2-E, a retinoid component of lipofuscin," *Invest. Ophthalmol. Visual Sci.* **41**, 2303–2308 (2000).
46. F. A. Shamsi and M. Boulton, "Inhibition of RPE lysosomal and antioxidant activity by the age pigment lipofuscin," *Invest. Ophthalmol. Visual Sci.* **42**, 3041–3046 (2001).
47. F. Schutt, B. Ueberle, B. Schnolzer, F. G. Holz, and J. Kopitz, "Proteome analysis of lipofuscin in human retinal pigment epithelial cells," *FEBS Lett.* **528**, 217–221 (2002).
48. F. Schutt, M. Bergmann, F. G. Holz, and J. Kopitz, "Proteins modified by malondialdehyde, 4-hydroxynonenal, or advanced glycation end products in lipofuscin of human retinal pigment epithelium," *Invest. Ophthalmol. Visual Sci.* **44**, 3663–3668 (2003).
49. M. Boulton, M. Rozanowska, B. Rozanowski, and T. Wess, "The photoreactivity of ocular lipofuscin," *Photochem. Photobiol. Sci.* **3**, 759–764 (2004).
50. C. Starita, A. A. Hussain, S. Pagliarini, and J. Marshall, "Hydrodynamics of ageing Bruch's membrane: implications for macular disease," *Exp. Eye Res.* **62**, 565–572 (1996).
51. R. D. Ross et al., "Presumed macular choroidal watershed vascular filling, choroidal neovascularization and systemic vascular disease in age-related macular degeneration," *Am. J. Ophthalmol.* **125**, 71–80 (1998).
52. A. B. Korenzwieg, "Changes in the choriocapillaries associated with senile macular degeneration," *Ann. Ophthalmol.* **9**, 753–764 (1977).
53. J. E. Grunwald, S. M. Hariprasad, and J. DuPont, "Effect of aging on the foveolar choroidal circulation," *Arch. Ophthalmol. (Chicago)* **116**, 150–154 (1998).
54. J. E. Grunwald et al., "Foveolar choroidal blood flow in age-related macular degeneration," *Invest. Ophthalmol. Visual Sci.* **39**, 385–390 (1998).
55. C. A. Curcio, C. L. Millican, K. A. Allen, and R. E. Kalina, "Aging of the human photoreceptor mosaic: Evidence for selective vulnerability of rods in central retina," *Invest. Ophthalmol. Visual Sci.* **34**, 3278–3296 (1993).
56. C. A. Curcio, C. Owsley, and G. R. Jackson, "Spare the rods, save the cones in aging and age-related maculopathy," *Invest. Ophthalmol. Visual Sci.* **41**, 2015–2018 (2000).
57. S. P. Sundelin, S. E. Nilsson, and U. T. Brunck, "Lipofuscin-formation in cultured retinal pigment epithelia cells is related to their melanin content," *Free Radic Biol. Med.* **30**, 74–81 (2001).
58. C. W. Spraul, G. E. Lang, and H. E. Grossniklaus, "Morphometric analysis of the choroid, Bruch's membrane, and retinal pigment epithelium in eyes with age-related macular degeneration," *Invest. Ophthalmol. Visual Sci.* **37**, 2724–2735 (1996).
59. J. Ambati et al., "An animal model of age-related macular degeneration in senescent Ccl-2- or Ccr-2-deficient mice," *Nat. Med.* **9**, 1390–1397 (2003).
60. M. F. Cordeiro et al., "Real-time imaging of single nerve cell apoptosis in retinal neurodegeneration," *Proc. Natl. Acad. Sci. U.S.A.* **101**, 13352–13356 (2004).